

# V<sub>2</sub>AlC, V<sub>4</sub>AlC<sub>3-x</sub> (x ≈ 0.31), and V<sub>12</sub>Al<sub>3</sub>C<sub>8</sub>: Synthesis, Crystal Growth, Structure, and Superstructure

Johannes Etzkorn, Martin Ade, and Harald Hillebrecht\*†

Institut für Anorganische und Analytische Chemie, Albert-Ludwigs-Universität Freiburg, Albertstrasse 21, D-79104 Freiburg, Germany, and Freiburger Materialforschungszentrum FMF, Stefan-Maier-Strasse 25, D-79104 Freiburg, Germany

Received February 28, 2007

Single crystals of V<sub>2</sub>AlC and the new carbides V<sub>4</sub>AlC<sub>3-x</sub> and V<sub>12</sub>Al<sub>3</sub>C<sub>8</sub> were synthesized from metallic melts. V<sub>2</sub>AlC was formed with an excess of Al, while V<sub>4</sub>AlC<sub>3-x</sub> (x ≈ 0.31) and V<sub>12</sub>Al<sub>3</sub>C<sub>8</sub> require the addition of cobalt to the melt. All compounds were characterized by XRD, EDX, and WDX measurements. Crystal structures were refined on the basis of single-crystal data. The crystal structures can be explained with a building-block system consisting of two types of partial structures. The intermetallic part with a composition VAl is a two-layer cutting of the hexagonal closest packing. The carbide partial structure is a fragment of the binary carbide VC<sub>1-x</sub> containing one or three layers. V<sub>2</sub>AlC is a H-phase (211-phase) with space group *P6<sub>3</sub>/mmc*, Z = 2, and lattice parameters of a = 2.9107(6) Å, and c = 13.101(4) Å. V<sub>4</sub>AlC<sub>3-x</sub> (x ≈ 0.31) represents a 413-phase with space group *P6<sub>3</sub>/mmc*, Z = 2, a = 2.9302(4) Å, and c = 22.745(5) Å. The C-deficit is limited to the carbon site of the central layer. V<sub>12</sub>Al<sub>3</sub>C<sub>8</sub> is obtained at lower temperatures. In the superstructure (*P6<sub>3</sub>/mcm*, Z = 2, a = 5.0882(7) Å, and c = 22.983(5) Å) the vacancies on the carbon sites are ordered. The ordering is combined to a small shift of the V atoms. This ordered structure can serve as a structure model for the binary carbides TMC<sub>1-x</sub> as well. V<sub>4</sub>AlC<sub>3-x</sub> (x ≈ 0.31) and V<sub>12</sub>Al<sub>3</sub>C<sub>8</sub> are the first examples of the so-called MAX-phases (MX)<sub>n</sub>MM' (n = 1, 2, 3), where a deficit of X and its ordered distribution in a superstructure is proven, (MX<sub>1-x</sub>)<sub>n</sub>MM'.

## Introduction

Binary carbides and nitrides of group IV and V transition metals are important high-temperature hard materials with extremely high melting points.<sup>1</sup> Recent investigations on ternaries such as Ti<sub>3</sub>SiC<sub>2</sub>,<sup>2</sup> Ti<sub>3</sub>AlC<sub>2</sub>,<sup>3</sup> Ti<sub>4</sub>AlN<sub>3</sub>,<sup>4</sup> and related compounds of the series (MX)<sub>n</sub>(MM') (M = "early" transition metal; M' = main group metal; X = C, N; n = 1, 2, 3).<sup>5</sup>

MAX-phases have shown excellent and unique material properties like damage and shock resistance or good thermal and electrical conductivity.<sup>6</sup>

Frequently, syntheses of high-melting compounds (T<sub>m</sub> ≈ 2000 K) are hindered by the low reactivity of the starting material. The application of high temperatures is the most simple strategy to overcome these problems, for example, by arc melting or induction heating, are not always an adequate solution because compounds with an incongruent melting point are difficult to achieve. Furthermore, phenomena like the formation of superstructures by ordering processes of vacancies or solid solutions can better be studied by using single crystals. The use of an additional metal (auxiliary metal technique<sup>7,8</sup>) enables formation and single-

\* To whom correspondence should be addressed. E-mail: harald.hillebrecht@ac.uni-freiburg.de. Phone: 0049-761-203 6131. Fax: 0049-761-203 6102.

† Albert-Ludwigs-Universität Freiburg.

- (1) (a) Freer, R., Ed. *The Physics and Chemistry of Carbides, Nitrides and Borides*; Kluwer Academic Publishers: Dordrecht, 1990. (b) Etmayer, P.; Lengauer, W. In *Encyclopedia of Inorganic Chemistry*; J. Wiley: Chichester, 1996; pp 519–531. (c) Toth, L. E. *Transition Metal Carbides and Nitrides*; Academic Press: New York, 1971. (d) Nowotny, H. *Angew. Chem.* **1972**, *84*, 973–982; *Angew. Chem., Int. Ed. Engl.* **1972**, *11*, 906–915.
- (2) (a) Barsoum, M. W.; El-Raghi, T. *J. Am. Ceram. Soc.* **1996**, *79*, 1953. (b) Barsoum, M. W.; El-Raghi, T. *Am. Sci.* **2001**, *89*, 334.
- (3) Tzenov, N. V.; Barsoum, M. W. *J. Am. Ceram. Soc.* **2000**, *83*, 825.
- (4) Rawn, C. J.; Barsoum, M. W.; El-Raghi, T.; Procopio, A. T.; Hoffmann, C. M.; Hubbard, C. R. *Mater. Res. Bull.* **2000**, *35*, 1785.
- (5) Barsoum, M. W. *Prog. Solid State Chem.* **2000**, *28*, 201.

(6) Barsoum, M. W.; Radovic, M.; Zhen, T.; Finkel, P.; Kalidindi, S. R. *Phys. Rev. Lett.* **2005**, *94*, 085501.

(7) (a) Lebeau, P. *C. R. Acad. Sci. (Paris)* **1898**, *127*, 393. (b) Scheel, H.; Elwell, D. *Crystal Growth from High-Temperature Solutions*; Academic Press: London, 1975.

(8) Kanatzidis, M. G.; Pöttgen, R.; Jeitschko, W. *Angew. Chem.* **2005**, *117*, 7156; *Angew. Chem., Int. Ed.* **2005**, *44*, 6996.

crystal growth of new ternary compounds which are not obtained by conventional high-temperature methods.<sup>9</sup>

The crystal structures of all compounds  $(MX)_n(MM')$  is based on layers of a closest packing of M and M' atoms with X atoms in octahedral voids between the M layers in a cubic stacking sequence. According to this building principle, mixed occupations for the metal atoms M/M', as well as for the nonmetals X (carbon and nitrogen), are possible. Furthermore, it is well-known for binary carbides and nitrides to form non-stoichiometric compounds with a C or N deficit.<sup>10,11</sup> In some cases, super structures by ordered vacancies are described.<sup>12</sup> Therefore, investigations of single crystals by means of X-rays and electron microprobe analysis give new insights into the structural properties, as compared to measurements on powder samples. For compounds of the system Ti/Al/Sn/C/N, we have shown on the basis of single-crystal investigations that substitutions of  $Al \leftrightarrow Sn$  and  $C \leftrightarrow N$  occur.<sup>13,14</sup>

In the system V/Al/C,  $V_2AlC$  was the only known ternary compound.<sup>15</sup> It was synthesized by arc melting and subsequent sintering (1000 °C). According to X-ray powder studies,  $V_2AlC$  was assigned to the hexagonal  $Cr_2AlC$  type<sup>16</sup> (H-phase) with  $a = 2.912 \text{ \AA}$  and  $c = 13.140 \text{ \AA}$ . Motivated by the unique material properties of the so-called MAX-phases<sup>5</sup> electrical transport, thermal transport, and elastic properties of several H-phases  $M_2AlC$  ( $M = Ti, V, Cr, Nb$ ) were measured.<sup>17</sup> Furthermore, the high-pressure behavior of  $V_2AlC$  was investigated up to 55 GPa.<sup>18</sup>

Recently, we have shown for the ternary system Ta/Al/C<sup>19</sup> that single crystals of  $Ta_3AlC_2$  and  $Ta_4AlC_3$  can be grown from Al and Al/Sn melts. Now we report on single crystal investigations on the H-phase  $V_2AlC$  and the C-deficient 413-phases  $V_4Al_{3-x}$  and  $V_{12}Al_3C_8$ , respectively.

## Experimental Section

**Syntheses, Crystal Growth, and Characterization.** Single crystals of  $V_2AlC$ ,  $V_4Al_{3-x}$  ( $x \approx 0.31$ ) (i.e.,  $V_4Al_{2.69}$ ), and  $V_{12}Al_3C_8$  were synthesized from melts of Al or Al/Co, respectively.

- (9) (a) Hillebrecht, H.; Gebhardt, K. *Z. Kristallogr. Suppl.* **2001**, *18*, 155. (b) Hillebrecht, H.; Ade, M. *Angew. Chem.* **1998**, *110*, 981–983; *Angew. Chem., Int. Ed.* **1998**, *37*, 935–938. (c) Hillebrecht, H.; Gebhardt, K. *Angew. Chem.* **2001**, *110*, 1492–1495; *Angew. Chem., Int. Ed.* **2001**, *40*, 1445–1447. (d) Meyer, F.; Hillebrecht, H. *J. Alloys Compd.* **1997**, *252*, 98–105. (e) Hillebrecht, H.; Meyer, F. *Angew. Chem.* **1996**, *108*, 2655–2657; *Angew. Chem., Int. Ed.* **1996**, *35*, 2499–2501.
- (10) Okamoto, H. *Phase Diagrams for Binary Alloys*; ASM International: Materials Park, OH, 2000.
- (11) Villars, P.; Calvert, L. D. *Pearson's Handbook, Crystallographic Data for Intermetallic Phases*; ASM International: Materials Park, OH, 1997.
- (12) (a) Kordes, D. *Phys. Stat. Sol. B* **1968**, *26*, K103–105. (b) Henfrey, A. W.; Fender, B. E. F. *Acta Crystallogr. B* **1970**, *26*, 1882–1883.
- (13) Ade, M. Ph.D. Thesis, University of Freiburg, Germany, 1997.
- (14) Lückeroth, H. Diploma thesis, University of Bonn, Germany, 1998.
- (15) Schuster, J. C.; Nowotny, H.; Vaccaro, C. *J. Solid State Chem.* **1980**, *32*, 213–219.
- (16) Jeitschko, W.; Nowotny, H. *Monatsh. Chem.* **1963**, *94*, 672–676.
- (17) Hettinger, J. D.; Lofland, S. E.; Finkel, P.; Meehan, T.; Palma, J.; Harrell, K.; Gupta, S.; Ganguly, A.; El-Raghy, T.; Barsoum, M. W. *Phys. Rev. B* **2005**, *72*, 115120.
- (18) Manoun, B.; Gulve, R. P.; Saxena, S. K.; Gupta, S.; Barsoum, M. W.; Zha, C. S. *Phys. Rev. B* **2006**, *73*, 024110.
- (19) Etzkorn, J.; Ade, M.; Hillebrecht, H. *Inorg. Chem.* **2007**, *46*, 1410–1418.

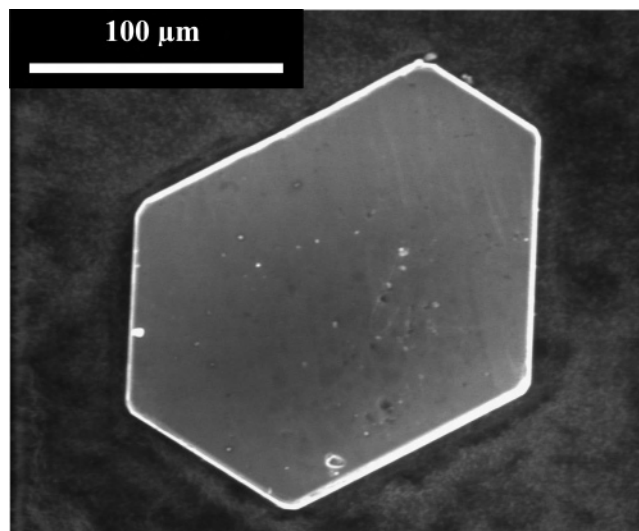


**Figure 1.** SEM picture of  $V_4Al_{3-x}$  ( $x \approx 0.31$ ).

Without the addition of Co, the only ternary compound observed was  $V_2AlC$ .  $VAL_3$  is the most prominent byproduct, but sometimes small amounts of  $V_7Al_{45}$  and  $VAL_{10}$  were additionally identified. The addition of Co resulted in  $Co_2Al_9$  and  $Co_4Al_{13}$  as byproducts and suppressed the formation of  $VAL_3$ . The amount of binary Co/Al phases varied. It is reduced by a longer duration of dissolution.  $V_2AlC$  was obtained at higher temperatures (1500–1650 °C), while  $V_4Al_{3-x}$  and  $V_{12}Al_3C_8$  were formed at lower temperatures (1300–1500 °C). Binary carbides of vanadium were never observed, but depending on the reaction conditions (ratio and purity of the elements, quality of the inert atmosphere, reaction of the crucible),  $Al_4C_3$  and  $Al_4O_4C$  were detected.

EDX and WDX measurements on single crystals were performed to ensure the correct composition. By EDX the ratio of V/Al was determined and the possible uptake of other metals (for example Co from the melt) was excluded. Furthermore, WDX measurements are necessary to exclude the incorporation of light elements with  $4 < Z < 13$ . Nitrogen is especially able to substitute carbon in *TM* carbides and cannot be reliably determined from X-ray data.

XRD patterns were recorded with a Siemens D5000 (Cu  $K_{\alpha 1}$  radiation, Ge monochromator, gas-filled PSD, Debye–Scherrer geometry, transmission). SEM pictures and EDX measurements were performed using a Jeol SM 6400 (Ge detector). For WDX investigations a Cameca SX 50 (analyzer crystal PC2, diamond and c-BN as standards) was used.

**$V_2AlC$ .** Without the use of Co, the main products were usually the intermetallic  $VAL_3$  and the H-phase  $V_2AlC$ . Single crystals of  $V_2AlC$  were obtained from the elements by the following procedure. Commercially available powders of the elements V (Acros, 99.5%), C (graphite, Chempur, 99.9+%), and Al (Riedel-de Haen, 99.9%) were intimately mixed in a ratio of 2:1:10 and pressed into a pellet (total mass: ca. 750 mg). The pellet was put into corundum crucibles and quickly (200 K/h) heated up to 1500 °C under an argon atmosphere. The sample was held for 50 h at 1500 °C, cooled to 1000 °C with a cooling rate of 5 K/h, held for 30 h, and then cooled at 30 K/h to RT. The excess metal of the solidified melt was removed by dissolving the regulus in half-concentrated aqueous HCl. The residue was washed and dried. Small hexagonal platelets were characterized as  $V_2AlC$ . The XRD pattern was indexed with a hexagonal unit cell with  $a = 2.9163(13) \text{ \AA}$  and  $c = 13.130(6) \text{ \AA}$ . Additional lines were assigned to  $VAL_3$ . EDX measurements on selected single crystals revealed a V/Al ratio of 70:30. WDX

**Table 1.** Structure Refinement of  $V_2AlC$ ,  $V_4AlC_{3-x}$  ( $x \approx 0.31$ ), and  $V_{12}Al_3C_8$ 

	$V_2AlC$	$V_4AlC_{3-x}$ ( $x \approx 0.31$ )	$V_{12}Al_3C_8$
cryst shape	hexagonal	hexagonal	hexagonal
cryst color	platelet metallic	platelet metallic	prism metallic
cryst size (mm <sup>3</sup> )	0.08 × 0.08 × 0.01	0.2 × 0.2 × 0.01	0.06 × 0.06 × 0.02
fw (g/mol)	140.87	262.76	788.3
cryst syst	hexagonal	hexagonal	hexagonal
space group	$P6_3/mmc$	$P6_3/mmc$	$P6_3/mmc$
lattice params	$a = 2.9107(6) \text{ \AA}$ $c = 13.101(4) \text{ \AA}$	$a = 2.9302(4) \text{ \AA}$ $c = 22.745(5) \text{ \AA}$	$a = 5.0882(7) \text{ \AA}$ $c = 22.983(5) \text{ \AA}$
cell vol (Å <sup>3</sup> )	96.12	169.12	515.30
formula units	2	2	2
density, calcd (g/cm <sup>3</sup> )	4.87	5.16	5.08
radiation	Mo $K_{\alpha 1}$	Mo $K_{\alpha 1}$	Mo $K_{\alpha 1}$
$\theta$ range	$-4 \leq h \leq 4$ $-4 \leq k \leq 4$ $-19 \leq l \leq 19$	$-4 \leq h \leq 3$ $-4 \leq k \leq 3$ $-34 \leq l \leq 34$	$-6 \leq h \leq 6$ $-7 \leq k \leq 7$ $-34 \leq l \leq 34$
temp (°C)	23	23	23
$2\theta_{\max}$	65°	64.6°	65.5°
diffractometer	IPDS II	IPDS I	IPDS I
	$0^\circ \leq \omega \leq 180^\circ$ $\psi = 0^\circ, 111^\circ$ $\Delta\omega = 2^\circ$	$0^\circ \leq \omega \leq 200^\circ$ $\Delta\omega = 2^\circ$	$0^\circ \leq \omega \leq 200^\circ$ $\Delta\omega = 2^\circ$
exposure time (s)	300	300	600
reflns measured	1079	1304	7404
independent	90	158	378
reflns			
reflns $I > 2\sigma(I)$	68	140	328
abs correction	empirical; equivalent method <sup>21</sup>	empirical; equivalent method <sup>21</sup>	empirical; equivalent method <sup>21</sup>
$R_{\text{int}}, R_\sigma$	0.0859, 0.0521	0.0539, 0.0214	0.0459, 0.0152
abs coeff (mm <sup>-1</sup> )	9.7	10.7	10.6
extinction coeff <sup>22</sup>	0.097(31)	0.009(3)	0.0155(13)
max./min. transmission	0.287; 0.083	0.1667; 0.0556	0.246; 0.105
structure solution	known model <sup>22</sup>	known model <sup>22</sup>	direct methods <sup>22</sup>
refinement	SHELXL 97 <sup>22</sup>	SHELXL 97 <sup>22</sup>	SHELXL 97 <sup>22</sup>
residual electron e <sup>-</sup> /Å <sup>3</sup>	+0.52, -0.70, 0.19	+0.50, -0.78, 0.12	+0.54, -0.61, 0.16
min, max, $\sigma$			
weighting	0.0595;	0.0183;	0.0476;
function <sup>22</sup>	0.0	0.2288	0.914
no. of params	9	16	26
$R$ factors	$R1(F) = 0.0295$ $wR2(F^2) = 0.0806$	$R1(F) = 0.0201$ $wR2(F^2) = 0.0432$	$R1(F) = 0.0277$ $wR2(F^2) = 0.0865$

investigations confirmed the presence of the elements V, Al, and C and the absence of N and O.

**$V_4AlC_{3-x}$  ( $x \approx 0.31$ ).**  $V_4AlC_{3-x}$  was obtained in a Co-containing melt. The elements V, C, Al, and Co (Chempur, 99.5%) were mixed in a ratio of 1.4:1:6.6:2 (total mass 750 mg) and submitted to the same temperature program as for the synthesis of  $V_2AlC$ .  $V_4AlC_{3-x}$  formed thin black hexagonal platelets with a metallic luster (thickness about 0.01 mm, diameter up to 0.2 mm (Figure 1)). The XRD pattern showed the lines of  $V_4AlC_{3-x}$  and  $Co_4Al_{13}$ . The refinement of the indexed reflections resulted in a hexagonal unit cell with  $a = 2.9276(14) \text{ \AA}$  and  $c = 22.69(2) \text{ \AA}$ . EDX measurements on selected single crystals revealed a ratio of 80:20 for V/Al and the absence of Co. WDX investigations confirmed the presence of the elements V, Al, and C and the absence of N and O.

**$V_{12}Al_3C_8$ .** Single crystals of the ordered  $V_{12}Al_3C_8$  were obtained by the application of lower temperatures. It is well known from binary transition metal carbides with a NaCl structure that ordering phenomena of the C atoms occur at temperatures between 1000 and 1200 °C.<sup>10</sup> The reaction conditions for  $V_{12}Al_3C_8$  were the same as those for  $V_4AlC_{3-x}$ , but the maximum temperature was 1300 °C. EDX measurements on selected single crystals revealed a ratio of 82:18 for V/Al and the absence of Co. WDX investigations confirmed the presence of the elements V, Al, and C and the absence of N and O.

**Table 2.** Coordinates, Displacement Parameters (in  $10^4 \text{ \AA}^2$ ), and Site Occupation Factors in  $V_2AlC^a$ 

atom	site	$x$	$y$	$z$	$U_{\text{eq}}$	sof <sup>b</sup>	$U_{11}$	$U_{33}$
V	4f	1/3	2/3	0.08558(7)	113(4)	0.994(6)	87(5)	165(5)
Al	2d	2/3	1/3	1/4	136(6)	0.96(4)	115(7)	176(11)
C	2a	0	0	0	125(13)	1.10(5)	86(16)	204(28)

<sup>a</sup> esd's in parentheses,  $U_{11} = U_{22} = 2 U_{12}$ ,  $U_{23} = U_{13} = 0$ . <sup>b</sup> In order to check for mixed occupations and/or vacancies, site occupation factors were treated by turns as free variables at the end of the refinement.

**Structure Determinations.  $V_2AlC$ .** A black hexagonal platelet was isolated from the Al melt and investigated using a single-crystal diffractometer equipped with an image plate detector (STOE, IPDS II, Mo  $K_{\alpha 1}$  radiation). All reflections were indexed with a hexagonal unit cell with lattice parameters of  $a = 2.9107(6) \text{ \AA}$  and  $c = 13.101(4) \text{ \AA}$ . Unit cell dimensions and reflection conditions ( $hkl$  with  $l = 2n$ ) were characteristic for a H-phase. The refinement was started with the parameters of a  $Cr_2AlC$  type<sup>16</sup> in space group  $P6_3/mmc$ .  $R$  factors of  $R1(F) = 0.0295$  and  $wR2(F^2) = 0.0806$  were obtained with 90 unique reflections (68 with  $I > 2\sigma(I)$ ) and 9 parameters. The refinement of the site occupation factors showed no significant deviations. Therefore, an ordered and stoichiometric structure can be assumed. Details are listed in Tables 1–3.



**Table 3.** Selected Distances (in Å) and Angles (in deg) in V<sub>2</sub>AlC<sup>a</sup>

V–C	2.0201(6) 3×	Al–Al	2.9107(6) 6×
V–Al	2.7321(9) 3×	Al–V	2.7321(9) 6×
V–V	2.8021(16) 3×	C–V	2.0201(6) 6×
V–V	2.9107(6) 6×	V–C–V	87.82(3)/92.18(3)

<sup>a</sup> esd's in parentheses.**Table 4.** Coordinates, Displacement Parameters (in 10<sup>4</sup> Å<sup>2</sup>) and Site Occupation Factors in V<sub>4</sub>AlC<sub>3-x</sub><sup>a</sup>

atom	site	x	y	z	U <sub>eq</sub>	sof	U <sub>11</sub>	U <sub>33</sub>
V1	4e	0	0	0.15504(2)	92(2)	1.004(4) <sup>b</sup>	83(2)	110(3)
V2	4f	1/3	2/3	0.05450(2)	120(2)	1.001(4) <sup>b</sup>	131(2)	99(3)
Al	2c	1/3	2/3	1/4	114(3)	0.975(9) <sup>b</sup>	113(4)	114(6)
C1	4f	2/3	1/3	0.10634(14)	87(6)	1.004(19) <sup>b</sup>	80(8)	111(11)
C2	2a	0	0	0	89(17)	0.692(23) <sup>c</sup>	80(19)	108(29)

<sup>a</sup> esd's in parentheses, U<sub>11</sub> = U<sub>22</sub> = 2U<sub>12</sub>, U<sub>23</sub> = U<sub>13</sub> = 0 <sup>b</sup> In order to check for mixed occupations and/or vacancies, site occupation factors were treated by turns as free variables at the end of the refinement <sup>c</sup> Free refinement (see text)

**Table 5.** Selected Distances (in Å) and Angles (in deg) in V<sub>4</sub>AlC<sub>3-x</sub><sup>a</sup>

V1–C1	2.022(2) 3×	V2–C1	2.062(2) 3×
V1–Al	2.7436(5) 3×	V2–C2	2.0973(4) 3×
V1–V2	2.8445(7) 3×	V2–V1	2.8445(7) 3×
V1–V1	2.9302(4) 6×	V2–V2	2.9302(4) 6×
		V2–V2	3.0010(7) 3×
Al–V1	2.7436(5) 6×	V2–C1–V2	88.3(1)
Al–Al	2.9302(4) 6×	V1–C1–V1	92.9(1)
C1–V1	2.022(2) 3×	V1–C1–V2	90.5(1)/178.3(1)
C1–V2	2.062(2) 3×	V2–C2–V2	88.6(1)
C2–V2	2.0973(4) 6×	V2–C2–V2	91.4(1)

<sup>a</sup> esd's in parentheses.

**V<sub>4</sub>AlC<sub>3-x</sub> (x ≈ 0.31).** A hexagonal platelet was isolated from the Al/Co melt, which had been heated up to 1500 °C. According to unit cell dimensions (*a* = 2.9302(4) Å, *c* = 22.745(5) Å), symmetry (Laue-class 6/*mmm*), and reflection conditions (*hkl* with *l* = 2*n*) the refinement was started in space group *P6<sub>3</sub>/mmc* with the structure model of a 413-phase.<sup>12,21</sup> The quick convergence of the refinement (158 reflections, 140 with *I* > 2σ(*I*), 16 parameters, R1(*F*) = 0.0258, wR2(*F*<sup>2</sup>) = 0.0625) confirmed its qualitative correctness, but the displacement parameter of the C1 atom on site 2a (0,0,0) was larger (a factor of 2.5) than the parameter of C2, despite its similar coordination. The free refinement of the C1 site occupation factor resulted in an occupation of 69(2)% and displacement parameters nearly equal to those of C2. Therefore, a partial occupation of C1 is assumed. Final *R* factors were R1(*F*) = 0.0201 and wR2(*F*<sup>2</sup>) = 0.0432. Details are listed in Tables 1, 4, and 5. The deficit for C2 has been confirmed for several single crystals. The data given above represent the results for the best refinement.

**V<sub>12</sub>Al<sub>3</sub>C<sub>8</sub>.** The investigation of single crystals of V<sub>4</sub>AlC<sub>3-x</sub>, which were grown from an Al/Co melt at a lower temperature of 1300 °C, showed weak super reflections. To index them it was necessary to enlarge the lattice parameter *a* by a factor of √3, so values of *a* = 5.0882(7) Å and *c* = 22.983(5) Å were obtained.<sup>23</sup> The Laue-class 6/*mmm* remained unchanged, but the reflection condition was *h0l* with *h* = 2*n*. The structure solution by direct methods was started in space group *P6<sub>3</sub>/mcm*. The structure model

yielded was very similar to V<sub>4</sub>AlC<sub>3-x</sub>, but the C atoms were ordered and all sites completely occupied with very small standard deviations. The final refinement with 378 independent reflections (328 with *I* > 2σ(*I*)) and 26 parameters gave *R*-values of R1(*F*) = 0.0277 and wR2(*F*<sup>2</sup>) = 0.0865. The U<sub>eq</sub> values are similar (especially C1 and C2) and the shape of the displacement ellipsoids are nearly isotropic. In connection with the EDX and WDX measurements, V<sub>12</sub>Al<sub>3</sub>C<sub>8</sub> should be considered as a completely ordered and stoichiometric compound. Details are listed in Tables 1, 6, and 7. For obvious reasons, the data set can also be refined with the structure of the subcell.<sup>24</sup>

Further details on the structure refinements (complete list of distances and angles, *F<sub>o</sub>/F<sub>c</sub>* list) may be obtained from: Fachinformationszentrum Karlsruhe, D-76344 Eggenstein-Leopoldshafen (Germany) (fax: +49)724-808-666; e-mail: crysdata@fiz-karlsruhe.de) on quoting the registry number CSD-416854 (V<sub>2</sub>AlC), CSD-416855 (V<sub>4</sub>AlC<sub>3-x</sub>), and CSD-416856 (V<sub>12</sub>Al<sub>3</sub>C<sub>8</sub>).

## Results and Discussion

**V<sub>2</sub>AlC.** The single-crystal investigations on V<sub>2</sub>AlC confirm and state more precisely the results of previous studies based on powder data. According to the crystal structure of a H-phase (or 211-phase) the metal atoms form a hexagonal closest packing with alternating sequences of two layers of vanadium atoms and one layer aluminum. The C atoms are in octahedral voids between the V layers (Figure 2). The distances within the layers are given by the lattice parameter *a* (2.9107(6) Å). The metal–metal distances between the layers are shorter (V–Al, 2.7321(9) Å; V–V, 2.802(2) Å). The C–V-distances of 2.0201(6) Å are about 5% shorter than in the binary VC (2.086 Å) but similar to V<sub>2</sub>C (2.030 Å), which is assigned to a defect NiAs type.<sup>25</sup> The CV<sub>6</sub> octahedra's "compression" in [001] directions results in V–C–V angles of 87.8° and 92.2°. Similar changes are also observed for other 211-phases like Cr<sub>2</sub>AlC,<sup>16</sup> Ti<sub>2</sub>GaC, Cr<sub>2</sub>GaC Ti<sub>2</sub>SnC, and Zr<sub>2</sub>SnC.<sup>22</sup>

**V<sub>4</sub>AlC<sub>3-x</sub> (x ≈ 0.31).** The structure of V<sub>4</sub>AlC<sub>3-x</sub> is analogous to the 413-phases as they are reported for Ti<sub>4</sub>Al<sub>1-x</sub>Sn<sub>x</sub>C<sub>1-y</sub>N<sub>y</sub> (x ≈ 0.18; y ≈ 0.85),<sup>14</sup> Ti<sub>4</sub>AlN<sub>3</sub>,<sup>4</sup> and Ta<sub>4</sub>AlC<sub>3</sub>.<sup>19,26</sup> The metal atoms form a sequence ABABACBCBC = (hhhcc)<sub>2</sub> with Al atoms in every fifth layer (bold letters) in a hexagonal sequence. The C atoms are located in octahedral voids which are formed exclusively by vanadium (Figure 3). In regular 413-phases, these layers represent a cutting of a NaCl structure type. In V<sub>4</sub>AlC<sub>3-x</sub>, the C position of the middle layer is partially occupied (69(2)%). The surroundings of all atoms can easily be derived from this building principle (anticuboctahedra for Al and V1, cuboctahedra for V2, octahedral for C1 and C2, three V1–C1 distances, six V2–C1/C2 distances). The V–C distances show a significant variation from 2.022(2) over 2.062(2) to

(24) R1(*F*) = 0.0223, wR2(*F*<sup>2</sup>) = 0.0676; V1: *z* = 0.15505(3), U<sub>eq</sub> = 0.0120(3), U<sub>11</sub> = 0.0119(3), U<sub>33</sub> = 0.0123(4); V2: *z* = 0.05452(4), U<sub>eq</sub> = 0.0149(3), U<sub>11</sub> = 0.0167(3), U<sub>33</sub> = 0.0113(4); Al: U<sub>eq</sub> = 0.0147(4), U<sub>11</sub> = 0.0155(6), U<sub>33</sub> = 0.0130(8); C1: *z* = 0.10545(16), U<sub>eq</sub> = 0.0118(7), U<sub>11</sub> = 0.0118(10), U<sub>33</sub> = 0.0118(16); C2: U<sub>eq</sub> = 0.0135(25), U<sub>11</sub> = 0.0114(27), U<sub>33</sub> = 0.0174(44).

(25) Bowman, A. L.; Wallace, T. C.; Yarnel, J. L.; Wenzel, R. G.; Storms, E. K. *Acta Crystallogr.* **1965**, *19*, 6–9.

(26) Manoun, B.; Saxena, S. K.; El-Raghi, T.; Barsoum, M. W. *Appl. Phys. Lett.* **2006**, *88*, 201902.

(20) Sheldrick, G. M. *SHELXL*; University of Göttingen: Göttingen, Germany, 1997.

(21) *XSHAPE*; STOE Cie: Darmstadt, Germany, 2003.

(22) Eitzkorn, J. Ph.D. Thesis, University of Bayreuth, Germany, 2002.

(23) The differences of the lattice parameters (especially the *c* axis) are frequently observed for single crystals grown at different temperatures.<sup>21</sup>

**Table 6.** Coordinates, Displacement Parameters (in  $10^4 \text{ \AA}^2$ ) and Site Occupation Factors in  $\text{V}_{12}\text{Al}_3\text{C}_8^a$ 

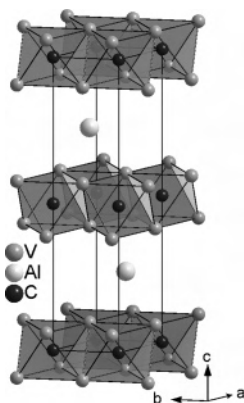
atom	site	x	y	z	$U_{\text{eq}}$	sof <sup>b</sup>	$U_{11}$	$U_{22}$	$U_{33}$
V1	4e	0	0	0.15309(4)	122(2)	1.000(5)	124(4)	$U_{11}$	119(4)
V2	8h	1/3	2/3	0.15601(3)	123(2)	0.999(4)	125(3)	$U_{11}$	119(3)
V3	12k	0.3525(1)	0	0.05451(2)	122(2)	0.995(5)	125(3)	121(3)	119(3)
Al	6g	0.3293(2)	0	1/4	154(4)	1.02(1)	162(5)	160(6)	138(7)
C1	12k	0.6679(5)	0	0.10638(14)	127(6)	1.00(3)	123(9)	135(11)	128(14)
C2	4d	1/3	2/3	0	136(9)	1.00(3)	126(13)	$U_{11}$	156(22)

<sup>a</sup> esd's in parentheses;  $U_{12} = 1/2 U_{22}$ ,  $U_{23} = U_{13} = 0$ ; exceptions: V3,  $U_{13} = 2(1)$ ; C1,  $U_{13} = -7(6)$ . <sup>b</sup> In order to check for mixed occupations and/or vacancies, site occupation factors were treated by turns as free variables at the end of the refinement.

**Table 7.** Selected Distances (in  $\text{\AA}$ ) and Angles (in deg) in  $\text{V}_{12}\text{Al}_3\text{C}_8^a$ 

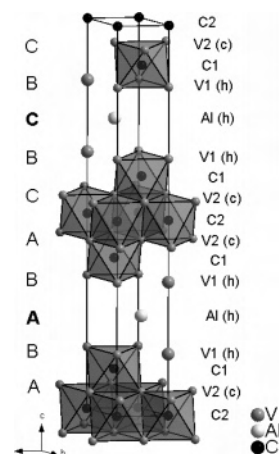
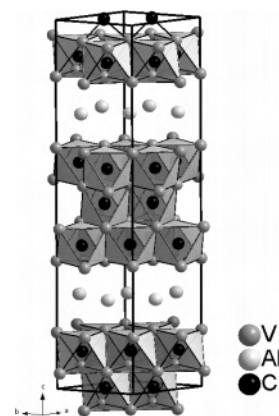
V1–C1	2.002(3) 3×	V3–C1	1.999(3)
V1–Al	2.787(1) 3×	V3–C2	2.071(1) 2×
V1–V3	2.890(1) 3×	V3–C1	2.113(2) 2×
V1–V2	2.938(1) 6×	V3–V2	2.857(1) 2×
		V3–V3	2.857(1) 4×
V2–C1	2.047(2) 3×	V3–V1	2.890(1)
V2–Al	2.753(1) 3×	V3–V3	2.921(1)
V2–V3	2.857(1) 3×	V3–V3	3.081(1) 2×
V2–V1	2.938(1) 3×	V3–V3	3.106(1) 2×
V2–V2	2.938(1) 3×		
Al–V2	2.753(1) 4×	C2–V3	2.071(1) 6×
Al–V	2.787(1) 2×	V3–C2–V3	87.2(1)/89.7(1) /
Al–Al	2.902(1) 2×		96.1(1)/175.3(1)
Al–Al	2.956(1) 4×		
C1–V3	1.999(3)	V3–C1–V3	88.0(1)/94.7(1)
C1–V1	2.002(3)	V1–C1–V2	93.1(1)
C1–V2	2.047(2) 2×	V2–C1–V2	91.7(1)
C1–V3	2.112(2) 2×	V2–C1–V3	86.7(1)/89.8(1)/177.3(1)
		V1–C1–V3	89.2(1)/175.8(1)

<sup>a</sup> esd's in parentheses; M–M distances of M atoms in the same layer are in italics.

**Figure 2.** Crystal structure of  $\text{V}_2\text{AlC}$  (H- or 211-phase).

2.0972(4)  $\text{\AA}$ . In the center, they are comparable to VC. This can be seen as an increase of the “flattening” of the  $\text{CV}_6$  octahedra on getting closer to the Al layers. The changes of M–M distances and V–C–V angles are in a line with this. Similar geometrical conditions were observed in  $\text{Ta}_4\text{AlC}_3$  with Ta–C distances of 2.17, 2.21, and 2.23  $\text{\AA}$  (Ta–C in TaC: 2.23  $\text{\AA}$ ). Also the increase of the lattice parameter  $a$  in  $\text{V}_4\text{AlC}_{3-x}$  compared to  $\text{V}_2\text{AlC}$  reflects the approach to the structure of the binary VC. A value of 2.950  $\text{\AA}$  is obtained by transformation of the cubic unit cell. Similar observations were made for the row  $\text{Ta}_2\text{AlC}$ ,  $\text{Ta}_3\text{AlC}_2$ , and  $\text{Ta}_4\text{AlC}_3$ .<sup>19</sup> Because the structure of  $\text{V}_4\text{AlC}_{3-x}$  is the disordered variant of  $\text{V}_{12}\text{Al}_3\text{C}_8$ , the detailed discussion of the crystal structure will be focused on  $\text{V}_{12}\text{Al}_3\text{C}_8$ .

**$\text{V}_{12}\text{Al}_3\text{C}_8$ .**  $\text{V}_{12}\text{Al}_3\text{C}_8$  is the first example of an ordered defect variant of a MAX-phase:  $(\text{MX}_{1-x})_n\text{MM}'$ . The general

**Figure 3.** Crystal structure of  $\text{V}_4\text{AlC}_{3-x}$  with  $x \approx 0.31$  (413-phase).**Figure 4.** Crystal structure of  $\text{V}_{12}\text{Al}_3\text{C}_8$ ; ellipsoids represent a probability of 99%.

principle of  $\text{V}_{12}\text{Al}_3\text{C}_8$  corresponds to the 413-phases (sequence of metal layers, C in octahedral voids of V, Figure 4). In the case of  $\text{V}_{12}\text{Al}_3\text{C}_8$ , one-third of the octahedral voids in the middle layer remain empty in an ordered way that a graphite-like layer of octahedra is formed (Figure 5). The  $\text{CV}_6$  octahedra are connected by common vertices. This motif is found as isolated layers in the layer structures of trihalides like  $\text{CrCl}_3$ ,  $\text{AlCl}_3$ , and  $\text{BiI}_3$ .<sup>27</sup>

The ordering of the defects causes a distortion of the  $\text{CV}_6$  octahedra of C1. There are two shorter distances (1.999, 2.002  $\text{\AA}$ ), two medium (2.047  $\text{\AA}$ ), and two longer (2.112  $\text{\AA}$ ). The V–C distances in the central layer (C2–V3) are longer (2.071  $\text{\AA}$ ), and the octahedral coordination of C2 remains nearly unchanged (Figure 6). Similar to stoichio-

(27) Wells, A. F. *Structural Inorganic Chemistry*, 5th ed.; Clarendon Press: Oxford, 1984.

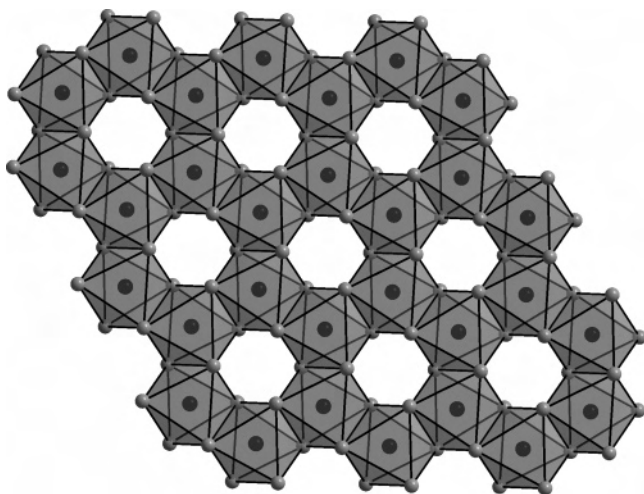


**Figure 5.** Central layer of  $CV_6$  octahedra at  $z = 0$  and  $0.5$ . Gray circles, V; black circles, C; squares, voids.

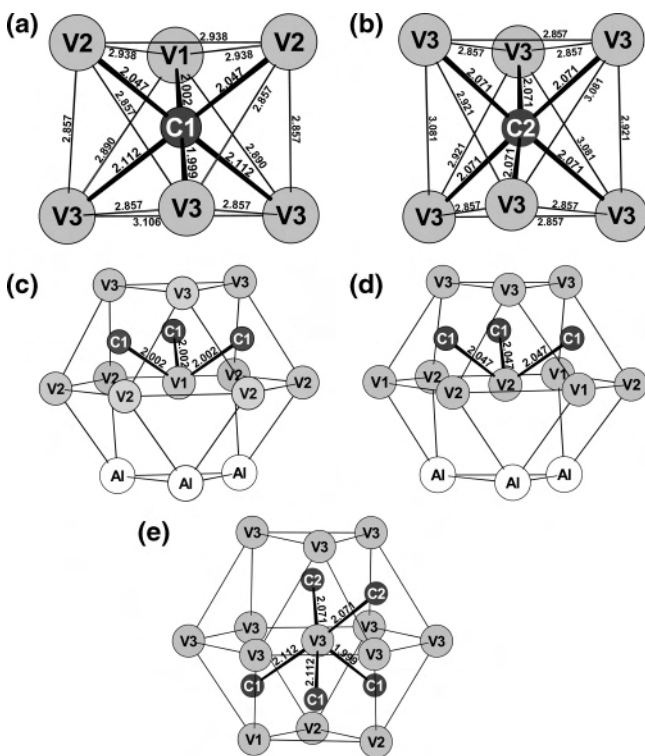


**Figure 6.** Coordination polyhedra in  $V_{12}Al_3C_8$ ; (a) C1, (b) C2, (c) V1, (d) V2, and (e) V3.

metric 413-phases, the average V–C distances in the “outer” layer (C1–V, 2.053 Å) are shorter than in the “inner” layers (C2–V3).

The surroundings of the metal atoms can easily be derived from the packing principle. The metal atoms form anticuboctahedra around Al, V1, and V2. Additionally there are three V–C bonds for V1 and V2 (Figure 6c and d). V3 is coordinated by five C atoms and a  $V_{12}$  cuboctahedron (Figure 6e). In general, the M–M distances between the layers are shorter than within them, where they correspond quite exactly to  $a/\sqrt{3}$ . Larger deviations are connected to the vacancies’ ordering that causes changes of the M–M distances too. The longest V–V distances of 3.081 and 3.106 Å are found around the free octahedral void.

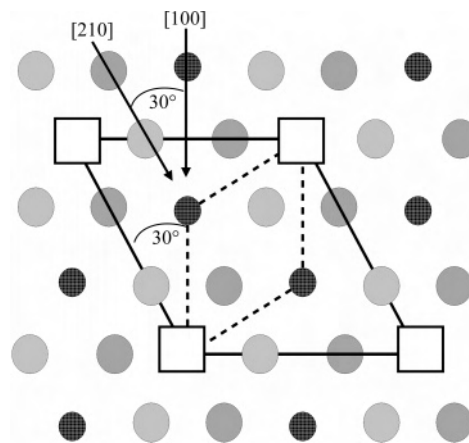


**Figure 7.** Relation between the subcell of  $V_4AlC_{3-x}$  ( $x \approx 0.31$ ) and the superstructure of  $V_{12}Al_3C_8$ , projection in the direction [001].

The calculation of the valence sum according to Brown<sup>28</sup> gives for C2 a value of 4.66 and for C1 a value of 4.93. This corresponds well the interpretation of  $V_{12}Al_3C_8$  as an intermediate between  $V_2AlC$  and VC where the valence sums are 5.35 and 4.47, respectively. For  $V_4AlC_{3-x}$ , the values are 4.91 (C1, outer layer) and 4.21 (C2, inner layer). The changes of the V–C distances by a shift of V atoms lead to an adjustment of the valence sums of the carbon atoms. The valence sums for the metal atoms confirm the intermediate position of  $V_{12}Al_3C_8$ . While the total values (V1, 6.03; V2, 5.87; V3, 6.91) reflect the increase of the V–C bonds (V1–C, 2.81; V2–C, 2.49; V3–C, 3.88), the intermetallic share decreases slightly (V1–M, 3.22; V2–M, 3.38; V3–M, 3.03). In agreement to this tendency, the valence sum vanadium are 6.37 in  $V_2AlC$  (V–C, 2.67; V–M, 3.70) and 7.34 in VC (V–C, 4.47; V–V, 2.87).

Figure 7 shows the geometrical relation between the subcell of  $V_4AlC_{3-x}$  and the superstructure of  $V_{12}Al_3C_8$ . The differences between both structures are very small. Besides the ordered arrangement of the C atoms in the middle layer (i.e., site 2a (0,0,0) in  $V_{12}Al_3C_8$  is free) the only significant deviations are small shifts of V3 (0.053 Å), V2 (0.022 Å), and V1 (0.044 Å antiparallel to V2). The shifts of V atoms correlate directly to the ordered C deficit. The shift of V3 is in the [100] direction away from the empty site. V2 is located above and below the C2 position and is away from this site (direction [001] while V1 is shifted in the opposite direction). Model calculations show that the intensities of the superstructure reflections depend mainly on the shifts of vanadium. Despite these small changes, the reflections defining the superstructure are clearly detected. Out of the total of 378 intensities observed (328 with  $I > 2\sigma(I)$ ), there are 162 from the subcell (146 with  $I > 2\sigma(I)^{23}$ ).

The examples of  $V_4AlC_{3-x}$  and  $V_{12}Al_3C_8$  show the advantages of single-crystal data compared to powder data. No reflection of the superstructure was detected in the powder pattern. The hints for the carbon deficit are very vague according to the small differences of the  $U_{eq}$  values. Therefore, the existence of a C deficit and the formation of a superstructure at lower temperatures would probably not

(28) Brown, I. D. *J. Appl. Crystallogr.* **1996**, *29*, 479–480.



be detectable by powder methods. In particular, the satisfying refinement of the superstructure demands single-crystal data.

The subcell of  $V_4AlC_{3-x}$  and the superstructure of  $V_{12}Al_3C_8$  are connected by a simple group–subgroup relation.<sup>29</sup> There is a transition (“klassengleich”) of order 3 ( $k3$ ) between  $P6_3/mmc$  and  $P6_3/mcm$  leading to super structure reflections and an enlargement of the unit cell ( $a' = \sqrt{3} a$ ), which is shown in Figure 7.

As outlined in the Experimental Section, the formation of  $V_4AlC_{3-x}$  and  $V_{12}Al_3C_8$  depends from the temperature (1500 and 1300 °C, respectively). According to this and the usual behavior of vacancies in solids,  $V_4AlC_{3-x}$  obviously represents a HT-phase and  $V_{12}Al_3C_8$  the LT-phase. The unambiguous proof of this relation and a direct observation of the transition is very difficult by DTA measurements because only small caloric effects and slow kinetics must be expected. As far as we know, a direct transition was not observed even for binary *TM* carbides  $TMC_{1-x}$ . Powder X-ray investigations are not possible because the X-ray powder diagram shows no superstructure reflections. Finally, single-crystal investigations including the detection of weak superstructure reflections at temperatures above 1000 °C are not easy.

**Relation to Binary Carbides  $TMC_{1-x}$ .** The determination of the ordered distribution of carbon in  $V_{12}Al_3C_8$  offers new aspects for the crystal structures of binary *TM* carbides with a carbon deficit  $TMC_{1-x}$ . The binary carbides of the “early” transition metals show unique properties like great hardness and high chemical and thermal stability.<sup>1</sup> Therefore, they are very important for applications as hard materials especially for composite materials (“cermets”).<sup>1</sup> Some of the compounds with lower C content represent stacking variants of closest sphere packings where the octahedral voids between hexagonal sequences remain free by geometrical reasons (for example  $M_2C$ ,  $M_3C_2$ ,  $M_4C_3$ <sup>30</sup>). In other cases with higher C content, the ordering variants are based on the cubic closest packing of the NaCl-type (for example  $V_8C_7$ ,  $V_6C_5$ ,  $Nb_6C_5$ <sup>10,11,30,31</sup>). Because of experimental reasons (low diffraction power of C, small single-crystal size, scattering length of V, high pseudosymmetry), structural parameters like V–C distances were usually derived by a geometrical construction (closest packing, regular  $CV_6$  octahedra) from lattice parameters and space group on the basis of data received by diffraction of X-rays, neutrons, and/or electrons, as well as (HR)TEM. To our knowledge,<sup>10,11</sup>  $V_8C_7$  is the only exception. A Rietveld analysis of X-ray data<sup>32</sup> revealed an ordered cubic structure ( $a = 8.34927(2)$  Å, space group  $P4_332$ ). Within the cubic closest packing of V atoms, one-eighth of the octahedral voids remains empty in a way that in each alternating layer one-sixteenth and three-sixteenths of the voids are occupied. One of the three different  $CV_6$  octahedra is strongly distorted with C–V distances between 1.79 and 2.58 Å (C3–V), while the other two (C1–V, 2.14

Å; C2–V, 1.98–2.12 Å) are comparable to the distances in  $V_{12}Al_3C_8$ . The distribution of C atoms (or voids, respectively) is given by the space group and therefore are without doubt, but the values for the C–V distances are very different than our results. The shifts of the V atoms of about 0.03–0.06 Å displaced from the ideal sites are comparable to  $V_{12}Al_3C_8$ . Obviously, the position of C3 is not located in the correct way by Rietveld refinement.

For  $V_6C_5$ , Venables et al.<sup>33</sup> presented a structure model in space group  $P3_1$  assuming a cubic close packing of vanadium and C in octahedral sites with idealized parameters (undistorted metal layers, C exactly in the center of the octahedra). Therefore, the space group was corrected to  $P3_121$  later on.<sup>34</sup> The ordered distribution of vacancies is the same as we observed in  $V_{12}Al_3C_8$ , i.e., between every second layer, one-third remains free in a way that a graphite-like pattern of corner-sharing octahedral is formed. The voids follow a  $3_1$  screw axis.

A similar structure is observed for monoclinic  $Nb_6C_5$  ( $C2/m$ ,  $a = 4.560$  Å,  $b = 9.457$  Å,  $c = 4.560$  Å,  $\beta = 109.47^\circ$ )<sup>35</sup> with the cubic closest packing of Nb and C in five-sixth of the octahedral voids, but here the voids follow the direction [001]. It should be noted that the same topological relations are observed for the  $CrCl_3$  type<sup>27</sup> ( $P3_121$ , ccp of Cl, Cr in two-thirds of the octahedral voids in every second layer). In monoclinic ( $C2/m$ )  $AlCl_3$ ,<sup>27</sup> the voids are arranged in the [001] direction.

## Conclusions

The use of molten metals enables access to single crystals of ternary carbides. Single crystals of the H-phase  $V_2AlC$  can be obtained from a V/Al melt. Single crystals of more complex compounds, so-called MAX-phases, can be grown by the auxiliary metal bath technique. For the system V/Al/C, it turns out that cobalt is a suitable auxiliary metal which is not taken up by the ternary compounds. At 1500 °C, a 413-phase  $V_4AlC_{3-x}$  ( $x \approx 0.31$ ) is produced. The deviation from the ideal composition results from the C deficit (occupation 69(2)%) in the central carbide layers. At a lower temperature of 1300 °C, an ordering process of the C vacancies leads to the formation of a superstructure which is combined to small but significant shifts of the V atoms. The resulting composition  $V_{12}Al_3C_8$  represents the first example of a MAX-phase  $(MX_{1-x})_nMM'$  ( $n = 1, 2, 3$ ) where defects for X atoms were detected and its ordered distribution characterized. Single-crystal data are essential for the unambiguous proof of the defects and the access to reliable structural parameters. The ordering process is similarly observed in binary carbides of the early transition metals. Recently, thermodynamic calculations using the CALPHAD program were performed for the system V/C.<sup>36</sup> Because detailed structure determinations for binary carbides  $TMC_{1-x}$

(29) (a) H. Bärnighausen, H. *MATCH Comm. Math. Chem.* **1980**, 9, 139–175. (b) Wondratschek, H., Müller, U., Eds. *International Tables for Crystallography*; Kluwer Academic Press: Dordrecht, 2004; Vol. A1.

(30) Yvon, K.; Parthe, E. *Acta Crystallogr. B* **1970**, 26, 149–153.

(31) Parthe, E.; Yvon, K. *Acta Crystallogr. B* **1970**, 26, 153–163.

(32) Rafala, D.; Lengauer, W.; Ettmayer, P.; Lipatnikov, V. *N. J. Alloys Comp.* **1998**, 269, 60–62.

(33) Venables, J. D.; Kahn, D.; Lye, R. G. *Phil. Mag.* **1968**, 18, 177–192.

(34) Cenxual, K.; Gelato, L. M.; Penzo, M.; Parthe, E. *Acta Crystallogr. B* **1991**, 47, 433–439.

(35) Gusev, A. I.; Rempel, A. A. *Phys. Stat. Sol. A* **1986**, 93, 71–80.

(36) Hu, J.; Li, Ch.; Wang, F.; Zhang, W. *J. Alloys Comp.* **2006**, 421, 120–127.

$V_2AlC$ ,  $V_4AlC_{3-x}$  ( $x \approx 0.31$ ), and  $V_{12}Al_3C_8$

with ordered defects are very rare and not reliable, the structure of  $V_{12}Al_3C_8$  can serve as a model. Band structure calculations are in progress.<sup>37</sup>

---

(37) Schroeder, M.; Hillebrecht, H. To be published.

**Acknowledgment.** Thanks are due to Bayerisches Geo-Institut (BGI, Universität Bayreuth) for the access to WDX measurements and to Detlev Krausse for his support.

IC700382Y